



OPEN ACCESS

EDITED BY

Manoj Khandelwal,
Federation University Australia, Australia

REVIEWED BY

Alfredo Satyanaga,
Nazarbayev University, Kazakhstan
Ying Yuan,
Hebei GEO University, China

*CORRESPONDENCE

Ashok Kumar,
✉ ashokmin@iitism.ac.in
Krzysztof Skrzypkowski,
✉ skrzypko@agh.edu.pl

RECEIVED 13 November 2025

REVISED 02 February 2026

ACCEPTED 12 February 2026

PUBLISHED 13 March 2026

CITATION

Kumar R, Kumar A, Kumar A, Pandit B,
Ram S, Ray S, Skrzypkowski K,
Zagórski K, Zagórska A, Stasica J and
Rak Z (2026) Assessment of cavity
formation in the crown during tunnel
excavation in the Himalayan region.
Front. Earth Sci. 14:1745569.
doi: 10.3389/feart.2026.1745569

COPYRIGHT

© 2026 Kumar, Kumar, Kumar, Pandit,
Ram, Ray, Skrzypkowski, Zagórski,
Zagórska, Stasica and Rak. This is an
open-access article distributed under
the terms of the [Creative Commons
Attribution License \(CC BY\)](https://creativecommons.org/licenses/by/4.0/). The use,
distribution or reproduction in other
forums is permitted, provided the
original author(s) and the copyright
owner(s) are credited and that the
original publication in this journal is
cited, in accordance with accepted
academic practice. No use, distribution
or reproduction is permitted which
does not comply with these terms.

Assessment of cavity formation in the crown during tunnel excavation in the Himalayan region

Rajit Kumar¹, Ashok Kumar^{2*}, Abhishek Kumar²,
Bhardwaj Pandit¹, Sahendra Ram³, Saunak Ray²,
Krzysztof Skrzypkowski^{4*}, Krzysztof Zagórski⁵, Anna Zagórska⁶,
Jerzy Stasica⁴ and Zbigniew Rak⁴

¹Department of Mining Engineering, Indian Institute of Technology (Banaras Hindu University), Varanasi, Uttar Pradesh, India, ²Department of Mining Engineering, Indian Institute of Technology (Indian School of Mines), Dhanbad, Jharkhand, India, ³Department of Mining Engineering, National Institute of Technology, Rourkela, Odisha, India, ⁴Faculty of Civil Engineering and Resource Management, AGH University of Krakow, Krakow, Poland, ⁵Faculty of Mechanical Engineering and Robotics, AGH University of Krakow, Krakow, Poland, ⁶Research Centre in Kraków, Institute of Geological Sciences, Polish Academy of Science, Krakow, Poland

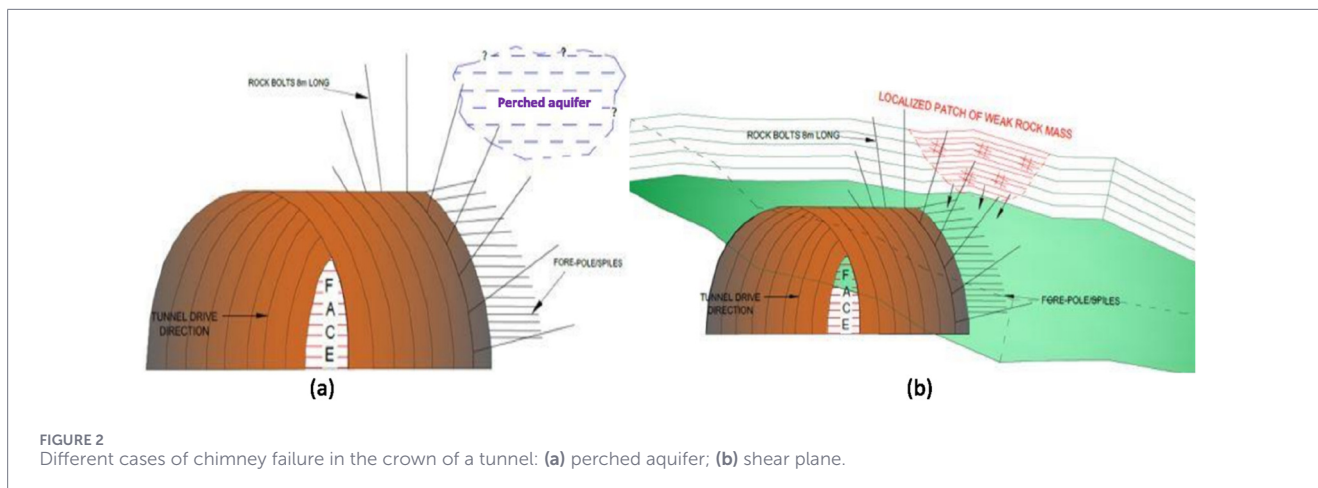
Chimney failure (crown displacement) in tunnel construction presents a critical concern of tunnelling projects in weaker rock formations at shallow depth of cover. Understanding the mechanisms and implications of chimney failure is of paramount importance for ensuring safe and efficient tunnel excavation, preventing potential hazards, and implementing effective remedial measures to maintain tunnel stability and structural integrity. An attempt has been made in this paper to simulate chimney failure in a tunnel and measured the vertical displacements and stresses in both unsupported and supported tunnels with cavities and compared with the field observations. This paper also discusses the importance of appropriate support strategies and remediation techniques to ensure the stability and structural integrity of tunnels while addressing challenges associated with crown displacement and cavity formation.

KEYWORDS

chimney failure, numerical simulation, roof bolt, shotcrete, support, tunnel

1 Introduction

Tunnels have been excavated for a wide range of purposes, serving the needs of road construction and water transportation for mining and civil construction projects. A conventional and time-tested technique, drilling and blasting, continues to excavate tunnels of various shapes and sizes. However, the Himalayas stand out as one of the most unstable regions on the planet, presenting immense challenges for underground excavations. This region's fragile geology, frequent tectonic activities and intricate geological structures make tunnelling endeavours exceptionally demanding. When undertaking excavation projects in the Himalayas, numerous hurdles are encountered, including the risk of rock bursts, difficult squeezing ground conditions, potential cavity failures, and water ingress. The phenomenon known as cavity failure, or chimney failure (Figure 1), emerges as a particularly significant issue during tunnel construction among these challenges, warrants an extensive research



tunnels while effectively addressing the challenges posed by cavity formation.

An attempt has been made in this paper to understand the mechanism of cavity formation in numerical models and proposed a support design as remedial measures based on analysis of vertical displacements and stresses to deal with such incidences.

2 Literature review

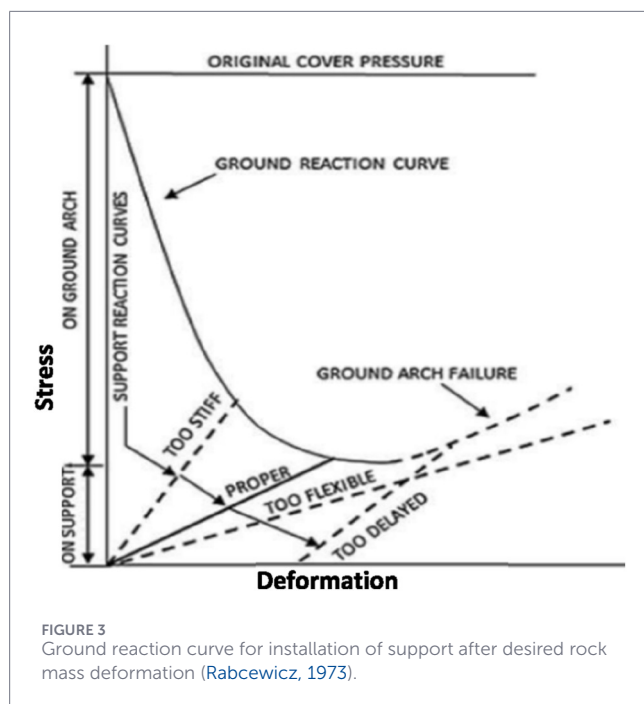
Tunnelling in the Himalayan region is often complicated by the presence of weak geological formations, high overburden stresses, and active tectonics. One of the major geotechnical challenges during tunnel excavation in this region is the formation of cavities in the crown area, often due to undetected weak zones, weathered rock mass, and sheared strata. These cavity formations pose significant risks to tunnel stability and construction timelines. Accurate and reliable predictions of rock deformation are essential in both civil and mining engineering projects involving rock masses (Abbas et al., 2024). Ensuring the precision of these forecasts is critical for optimizing structural design, enhancing safety, and enabling efficient planning and execution of excavation activities (Koopialipoor et al., 2022). In the beginning, tunnel stability was assessed using empirical approaches (Yang et al., 2021) and rock mass classification systems (Bieniawski, 1993). Nowadays, the deformation of the rock mass around the tunnel crown and walls are being analysed through numerical modelling techniques (Leu et al., 2001; Schmidt et al., 2010; Kumar, 2023).

Ground reaction curve (Figure 3) gives an idea of the support load capacity to be designed along with the permissible level of roof deformation (Rabcewicz, 1973). Schmidt et al. (2010) studied the factors influencing tunnel safety and behaviour of micropile umbrella and carried out 3D numerical simulation and analysis to investigate the effects of a micropile umbrella on the stability of tunnel of Burgos (Spain) constructed in miocenic sand clay. Schmidt et al. (2010) presented a 3D numerical analysis to investigate the effect of a micropile umbrella on the stability of the tunnel face. It was found that the micropiles should be installed as parallel as possible to the tunnel axis, minimising the pile angle.

The length of the pile should not be too long in order to avoid high bending moments, which can exceed material resistance and produce failure. The separation of the piles should not permit soil collapse between the pile tubes. As well as the overlapping of the single umbrellas with each other in order to secure a forerunning support: it should be chosen in a matter to grant a mutual support between the umbrella segments. Beg et al. (2025) highlighted that Himalayan tunnel projects face severe stability issues due to complex geology such as thrust and shear zones, folding, and intense *in situ* stresses along with challenging climatic and hydrological conditions. These factors drive common problems like rock bursts in deep overburden, squeezing in weak schistose mass, and significant water inflows, all of which escalate project cost and timeline. It emphasized that successful tunnelling in this region requires a holistic approach combining detailed geological investigations, adaptive construction techniques, and engineered support systems.

Under most conditions, tunnelling causes a transfer of the ground load by arching to sides of the opening, termed the ground-arch effect. The horseshoe shape is generally preferred for all but the weakest rocks, since the flat bottom facilitates hauling. By contrast, the stronger and more structurally efficient circular shape is generally required to support the greater loads from soft ground. Ability of roof to remain standing after excavation in underground mine is necessary to install a temporary or permanent support and remove the material. It is affected by the nature of rock mass and its parameters and also excavation technique. A number of scientists (Laufer, 1958; Bieniawski, 1993; Barton et al., 1975) have worked over the stand-up time of roof and proposed the width of unsupported excavation during construction of tunnel. Chimney failure has been found to be mainly occurring due to tunnelling operations in weak ground at shallow depth of cover. It is very difficult to predict such circumstances unless a comprehensive mapping of the site is carried out in advance. It is not related to stand-up time of roof (Laufer, 1958) (Figure 4). Ground reaction provides an idea of the supporting of the roof.

Upadhyay et al. (2023) reported the formation of a cavity between RD 312–320 m during the drivage of Adit-2 at the Rammam III Hydroelectric Project in the Sikkim Himalayas, attributed to a weathered, weak, or sheared zone located above the crown level, which remained undetected during excavation.



By systematically applying mitigation measures guided by the DRESS (Drainage–Reinforcement–Excavation–Support–Solution) philosophy, the project team successfully navigated through the problematic stretch and reached the rock face at RD 320 m. The adopted approach effectively mitigated loose rock falls and cavity formation triggered by high pore water pressure and a sheared rock mass. Stabilization in the cavity-prone section was achieved using drainage holes, steel ribs, shotcrete, and forepoling. According to Diwakar et al. (2022), the presence of complex geological features such as faults, folds, and shear zones makes the Himalayas one of the most challenging regions in the world for underground excavation projects. Ahmed et al. (2025) studied influencing factors affecting ground deformation during construction of Khari-Banihal Railway Tunnel (KBRT) in the geologically disturbed Western Himalayas and developed a predictive model using real-time 3D monitoring data and multiple linear regression (MLR) techniques. Li et al. (2020) conducted numerical simulations to assess the performance of tunnel linings in the presence of surrounding rock cavities. Their findings revealed that such cavities significantly impact tunnel stability and can lead to structural damage, with cavity width exerting a more pronounced effect on the tunnel's stress state than cavity depth.

Spyridis and Bergmeister (2024) studied the environmental impacts of tunnel construction which can be significantly reduced by optimizing the design and materials of the primary and secondary linings. Shen et al. (2014) discussed the 2008 Wenchuan earthquake in China which destroyed a number of tunnels to different degrees of the vulnerability, which stopped the emergency lifeline supply from the safety places. Huang et al. (2022) carried out the resilience analysis modelling of the underground infrastructure both at structural and system level due to man-made or natural hazards arising from climate change.

Cavity formation at the crown during Himalayan tunnel drivage is a multifaceted problem stemming from geological complexity,

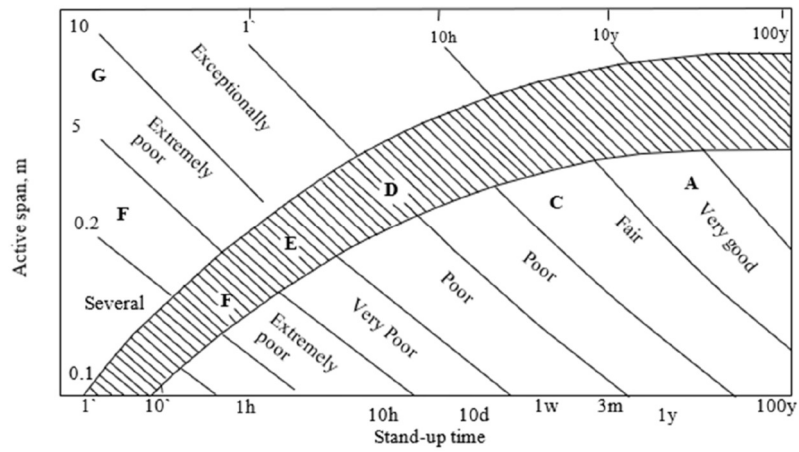
hydrological pressure, stress redistribution, and dynamic loading. A robust engineering response integrates detection, adaptive support, and excavation sequencing tailored to each tunnel. This integrative framework with proven success in real-world Himalayan projects, provides a blueprint for future works in similar settings.

3 Field study

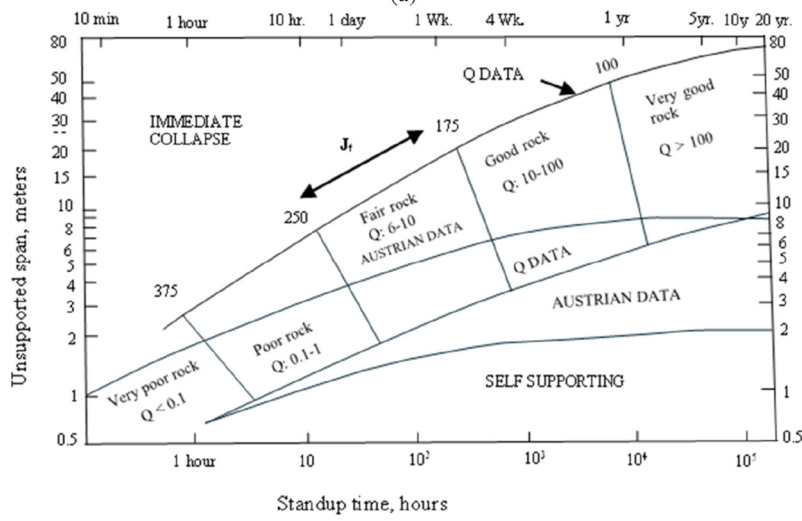
The work of four lane road from the end of Pandoh bypass to the Takoli section of National Highway-21 from 221.305 km to 242.000 km in the State of Himachal Pradesh, started in 2017 (Figure 5). Around 21.4 km of underground highway tunnels (4 twin tunnel, 2 single tube and cross-passage between LHS and RHS Tunnel), 3 major bridges, 10 minor bridges, 1 elevated bridge, 48 culverts, and 13 km of highways (including 290 m cut and cover section) has been constructed in the most challenging Pandoh-Takoli section of NH-21 (Figure 5). The tunnel is horseshoe shaped having width of 13.20 m, height of 7.90 m and length of 2053 m (Figure 6). The distance between the two twin tube tunnels is 34 m (Figure 7). The length of the RHS and LHS tube is 2,144.452 m and 2,142.663 m respectively. Peak overburden is around 250 m (RHS) and there are no peak overburden data available for LHS due to missing topographical surveys. The estimated peak overburden varying in the range of 300–350 m. The tunnels are being constructed in an alteration of meta-sediments belonging to the Haimanta Formation (Precambrian to Cambrian age). The average thickness of single layers is in the range of centimetres to a few meters. The discontinuities of the rock mass are mainly widely spaced (range of spacing: close to very wide). Details of wedge-cut drilling and blasting pattern adopted for tunnel excavation is shown in Figure 8. Rock support system for different nature of rock during tunnel excavation is mentioned in Table 1. The selected tunnel section represents a typical Himalayan tunnelling scenario characterised by shallow overburden, weak and sheared zones above the crown, and drill-and-blast excavation. These site-specific conditions directly contributed to cavity formation, making this project a representative case for the analysis of chimney failures.

4 Numerical simulation

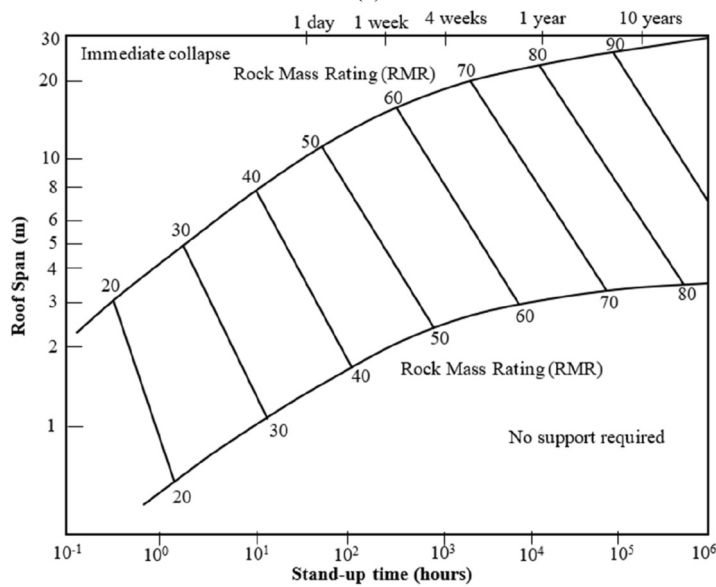
Numerical modelling is an important and popular tool to study the geotechnical problems. A model is created for developing a tunnel length of 50 m (Figure 9a) and the geological profile of the GT 3 and GT13 rock characteristics (Tables 2, 3) has been modelled (Figure 9b). The overburden above the tunnel is assumed to be constant. A draw of 1.25 m is considered by rock class of GT 3 and GT13. Drilling and blasting achieved a pull of 2.5 m in each round; therefore, tunnel is developed in the model at a distance of 2.5 m sequentially. *In-situ* stresses are initialised in the model as per the measurements of the site available. The primary aim of this study is to measure displacement on the crown, stresses, shear failure around the tunnel. Observations were made along the entire length of the tunnel without support. After observing the condition of sequentially developed tunnel, rock bolts (Table 4), steel ribs (Table 5) and a shotcrete liner (Table 6) were installed. After installation of supports, vertical stresses and



(a)



(b)



(c)

FIGURE 4 Stand-up time based on active span: (a) after Lauffer (1958); (b) after Q-system (Barton et al., 1975); (c) after Bieniawski (1993).

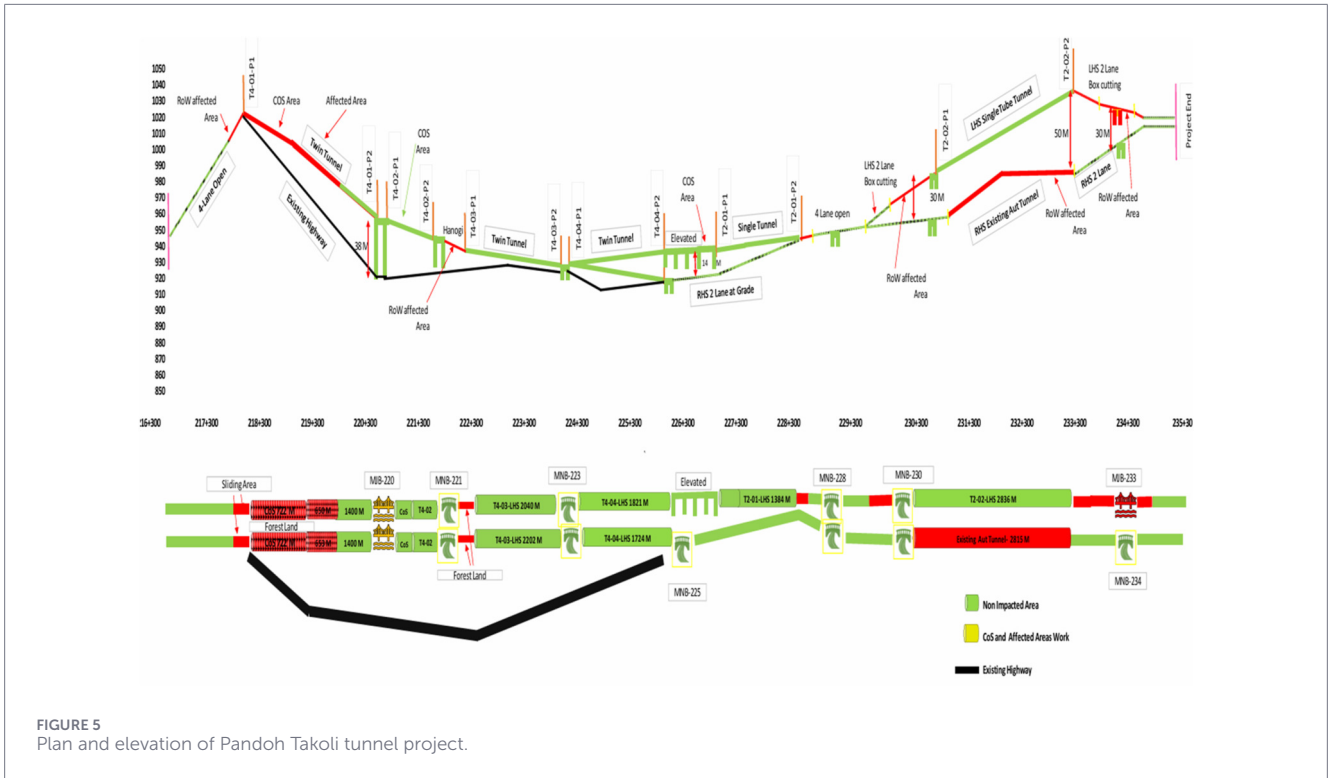


FIGURE 5 Plan and elevation of Pandoh Takoli tunnel project.



FIGURE 6 Sequential excavation and face supporting during tunnel excavation.

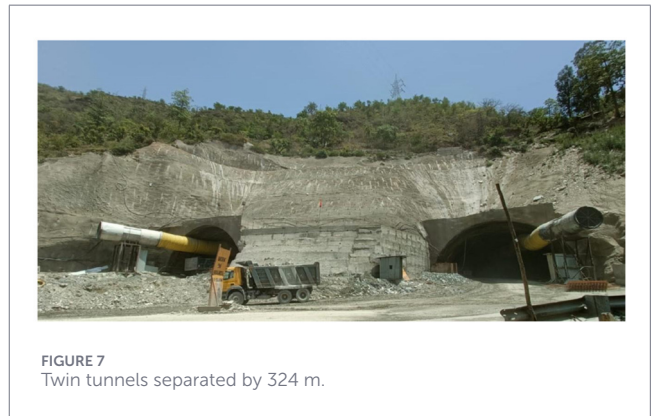


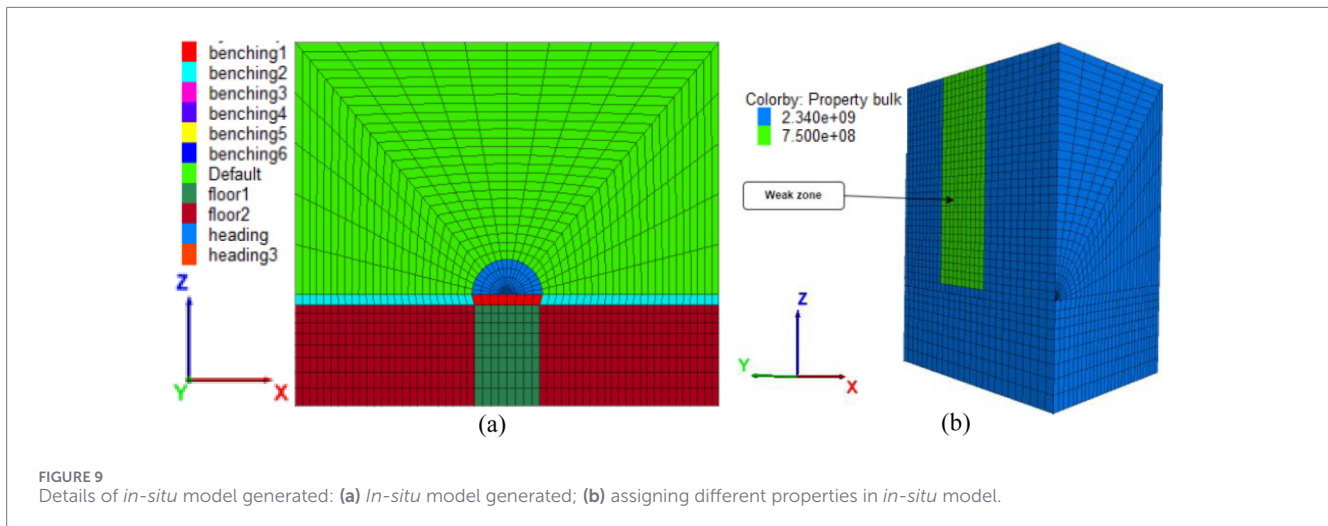
FIGURE 7 Twin tunnels separated by 324 m.

displacement were observed on the crown around the entire length of the tunnel.

The steps of modelling consisted of.

- a. Generation of radial cylindrical brick of size with 84 m and 50 m along x (−42 to 42) and y (0–50)- axes with 50 m roof and 20 m floor.
- b. Generation of boundary of the semi-circular tunnel (radius = 7.0) to be excavated.

- c. Group the developed geometry into various zones, i.e., heading 1, heading 2, heading 3, benching 1, benching 2, benching 3, benching 4, benching 5, benching 6, floor 1 and floor 2.
- d. Assigning Mohr-Coulomb constitutive material model properties to these zones. Applying the rock properties GT3 (bulk modulus- 2.083 GPa, shear modulus- 960 MPa, density- 2,750 kg/m³, cohesion- 0.224 MPa, angle of friction- 42°, tension- 0.6 MPa). Applying the rock properties GT13 to a weaker chimney zone (bulk modulus- 0.750 GPa, shear modulus- 346 MPa, density- 2,750 kg/m³, cohesion- 0.90 MPa, angle of friction- 23°, Tension- 0.6 MPa).
- e. Applying boundary conditions (left, right, front, back, and bottom faces).
- f. Initializing the vertical and horizontal stresses with required gradient.



Continuous crown displacement causing chimney formation during tunnel sequential excavation in the numerical model is shown in Figure 14.

In the numerical simulations, the support system was represented using built-in structural elements available in the simulation software package, namely, roof bolts (cable elements), steel ribs (beam elements), and shotcrete liners (liner/shell elements). These support elements are not governed by rock mass constitutive models such as Mohr–Coulomb or Hoek–Brown. Instead, they are simulated using dedicated structural constitutive laws specifically developed to represent the mechanical behaviour of support systems. Roof bolts were modelled using cable elements, which follow a one-dimensional axial elastic–plastic constitutive law combined with a bond–slip interaction at the grout–rock interface. The steel bar behaves linearly elastic up to the yield force and exhibits perfectly plastic behaviour beyond yielding. Load transfer between the bolt and surrounding rock is represented by shear coupling springs, which follow a linear elastic bond law and fail once the bond strength is exceeded, allowing for debonding and pull-out behaviour. Steel ribs were simulated using beam elements governed by elastic or elastic–perfectly plastic beam constitutive laws. In conditions where the ribs are sufficiently stiff and yielding is not expected, a linear elastic beam model was adopted. For yielding steel ribs in squeezing ground conditions, an elastic–perfectly plastic structural beam model was used, enabling the development of plastic hinges and redistribution of internal forces. Shotcrete support was modelled using liner (shell) elements, which behave as a two-dimensional continuum rather than a one-dimensional structural member. The liner was primarily simulated using a linear elastic constitutive model, which is commonly adopted in practice. The formulation allows the capture of key failure mechanisms such as tensile cracking, compressive yielding, and bending failure, depending on the stress state developed in the liner. Overall, the support system was simulated using structural elements governed by axial and bending elastic–plastic constitutive laws with appropriate interface coupling, providing a realistic representation of support–rock interaction without employing rock mass constitutive models for the supports. The mechanical properties and installation sequence of these support

components were assigned based on field specifications (Tables 4–6) to realistically capture rock–support interaction during sequential excavation.

Although cavity formation during Himalayan tunnel excavation is influenced by hydrological pressure and blast-induced dynamic loading, the present numerical simulations adopt a quasi-static framework to isolate the dominant role of geological weakness and stress redistribution in progressive crown cavity development. The weakening effects of groundwater are incorporated through reduced rock mass parameters, while blasting-induced disturbance is represented by staged excavation and stress release. Explicit hydro-mechanical and dynamic analyses are identified as important extensions for future work.

5 Analysis

The monitoring of the crown was carried out using extensometers at different point along the section of the tunnel (Figure 15) and these observations were used to calibrate the numerical model and predict the roof/side deformation during different stages of tunnel excavation. The displacement graph (Figure 16a) illustrates the initial stages of excavation, specifically the displacement of the crown's top surface around the tunnel portal. In the beginning of tunnel excavation, there is a noticeable rise in vertical displacement, indicating ground movement. However, as the excavation advances to a certain distance, the amount of vertical displacement saturated depicting equilibrium or stabilizes. The introduction of support during this phase effectively controlled the crown displacement, demonstrating the effectiveness of the support system in maintaining stability. However, the analysis of the displacement graph reveals that the existing support system, as depicted in Figure 16a does not effectively control the displacement of the crown. Consequently, additional support measures are necessary to ensure the stability of the tunnel. This can be attributed to the presence of weaker rock, which demands additional support to maintain stability. The graph (Figure 16a) clearly demonstrates that, in the absence of enhanced support, crown displacement continues, increasing the risk of tunnel instability or potential failure.

TABLE 2 Rockmass properties for GT3 and GT13 rock types.

Key parameters	Ground type			
	GT 1	GT 2	GT 3	GT 13
Rock type	Bedrock	Bedrock	Bedrock	Fault rock
UCS - intact rock (MPa)	30–60	30–60	30–60	Variable
Discontinuity spacing (cm)	>60	<20	<20	NA
Lithology	Alternation of slate to phyllites and metasilt to metasandstone; quartzite; locally thin interlayers of shale	Alternation of slate to phyllites and metasilt to metasandstone; quartzite; locally thin interlayers of shale	Alternation of slate to phyllites and metasilt to metasandstone; quartzite; locally thin interlayers of shale	Fault rock originating from various rock types
Description	Moderately to poor interlocking rockmass, medium to high strength, closely jointed; spacing: > 60 cm; large prismatic to tabular rock blocks (>60 cm)	Moderately to poor interlocking rockmass, medium to high strength, closely jointed; spacing: 20–60 cm; small tabular rock blocks (20–60 cm)	Moderately to poor interlocking rockmass, medium to high strength, closely jointed; spacing: > 60 cm; large prismatic to tabular rock blocks (>60 cm)	Heterogeneous fault rock, very closely to extremely fractured and/or sheared rock, without any or poor interlocking of blocks. Size of rock fragments from cobbles to gravel; occasionally with sandy to clayey matrix
Additional parameters — intact rock				
Specific gravity (kN/m ³)	27	27	27	-
Young's modulus (GPa)	20–30	20–30	20–30	-
Coefficient of elasticity	0.25	0.25	0.25	-
Indirect tensile strength (by brazilian test) (MPa)	3–18	3–18	3–18	-
Mi (Hoek-Brown constant)	5–10	5–10	5–10	-
Abrasivity (CAI)	1–4	1–4	1–4	-
Additional parameters — joints, cleavage				
Friction angle	27–37	27–37	25–35	Variable
Residual friction angle	23–35	23–35	20–30	Generally low
Roughness	Smooth-rough, planar	Smooth-rough, planar	Smooth-rough, planar	Generally smooth
Additional parameters — rockmass				
RQD	>70	>30	<40	NA
GSI	55–70	45–55	35–50	26
UCS (rockmass)	7.5–11	6–7.5	4.5–6	0.8–1.5
Cohesion	2–3	1.7–2.3	1.5–2	18–23
Angle of internal friction (°)	29–33	26–29	23–26	0.7–2.5
Young's modulus (GPa)	9–16	5–9	2.5–5	0.3

The examination of the displacement graphs (Figures 16b,c) reveals a significant increase in the value of crown deformation as compared to previous graphs (Figure 16a). The existing support system proved to be inadequate in controlling the displacement, ultimately resulting in cavity failure approximately 26 m from the tunnel portal. This indicates that either the ground conditions or the implemented support measures are insufficient to withstand the forces and pressures exerted on the tunnel walls. The occurrence of cavity failure (Figure 16c) signifies a collapse or deformation of the surrounding rock, posing a considerable risk to the overall stability of the tunnel. It is important to note that the interpretation of the graphs may vary without specific numerical values or additional

context. When assessing tunnel stability, it is crucial to consider other factors such as geological conditions, engineering design, and construction methods.

A clear correlation is observed between field-monitored crown displacement (Figure 15), weak geological conditions identified above the crown (Tables 2 and 3), and the limitations of the installed support system (Tables 4–6). Despite support installation, continued displacement was recorded, indicating insufficient confinement in the weak GT13 zone. Numerical results corroborate these observations, showing progressive deformation leading to cavity formation, thereby confirming the inadequacy of the existing support system under the prevailing geological conditions.

TABLE 3 General categories of different ground behaviour types.

Basic categories of behaviour types		Description of potential failure modes/mechanisms during excavation of the unsupported ground
GT 1	Stable	Stable ground with the potential of small local gravity induced falling or sliding of blocks
GT 2	Potential of discontinuity-controlled block all	Voluminous discontinuity controlled, gravity induced falling and sliding of blocks, occasional local shear failure on discontinuities
GT 3	Shallow failure	Shallow stress induced failure in combination with discontinuity and gravity-controlled failure
GT 4	Voluminous stress induced failure	Stress induced failure involving large ground volumes and large deformation
GT 5	Rock burst	Sudden and violent failure of the rock mass, caused by highly stressed brittle rocks and the rapid release of accumulated strain energy
GT 6	Buckling	Buckling of rocks with a narrowly spaced discontinuity set, frequently associated with shear failure
GT 7	Crown failure	Voluminous overbreak in the crown with progressive shear failure
GT 8	Raveling ground	Flow of dry or moist, intensely fractured, poorly interlocked rocks or soil with low cohesion
GT 9	Flowing ground	Flow of intensely fractured, poorly interlocked rocks or soil with high water content
GT 10	Swelling ground	Time dependent volume increase of the ground caused by physical chemical reaction of rock and water in combination with stress relief, leading to inward movement of the tunnel perimeter
GT 11	Ground with frequently changing deformation characteristics	Combination of several behaviours with strong local variations of stresses and deformations over longer sections due to heterogeneous ground (i.e., in heterogeneous fault zones; block-in matrix rock, tectonic mélanges)

TABLE 4 Roof bolts details used as the support system.

Yielding load (kN)	Length (m)	Diameter (mm)	Area (m ²)	Young's modulus (kN/m ²)	Axial stiffness (kN/m)	Spacing (m)	Bond strength (MN/m)	Perimeter bolt length (m)
250	6	32	4.7 x 10 ⁻⁴	2.1 x 10 ⁸	9.87 x 10 ⁴	1.25 (roof); 2.5 (perimeter)	0.1	6

TABLE 5 Steel ribs details used as the support system.

Steel ribs spacing (m)	Section depth (m)	Area (m ²)	Moment of inertia (kg-m ²)	Young's modulus (MPa)	Poisson's ratio	Compressive strength (MPa)	Tensile strength (MPa)
1	0.136	1.02 x 10 ⁻³	3.56 x 10 ⁻⁶	2.1 x 10 ⁵	0.30	400	250

TABLE 6 Shotcrete properties as the support system.

Thickness (cm)	Young's modulus (GPa)	Compressive strength (MPa)	Tensile strength (MPa)	Strength (MPa) with time
10	10-50	30-70	3-7	0.1-0.5 (6 min); 2-20 (24 h) 30-35 (7 days); 30-70 (28 days)

6 Discussion

The present study offers valuable insights into the mechanism of chimney (cavity) failure in tunnels excavated under weak and

heterogeneous Himalayan geological conditions, by integrating field observations with calibrated numerical simulations. The discussion below interprets the results in the context of geological controls, displacement behaviour, support system

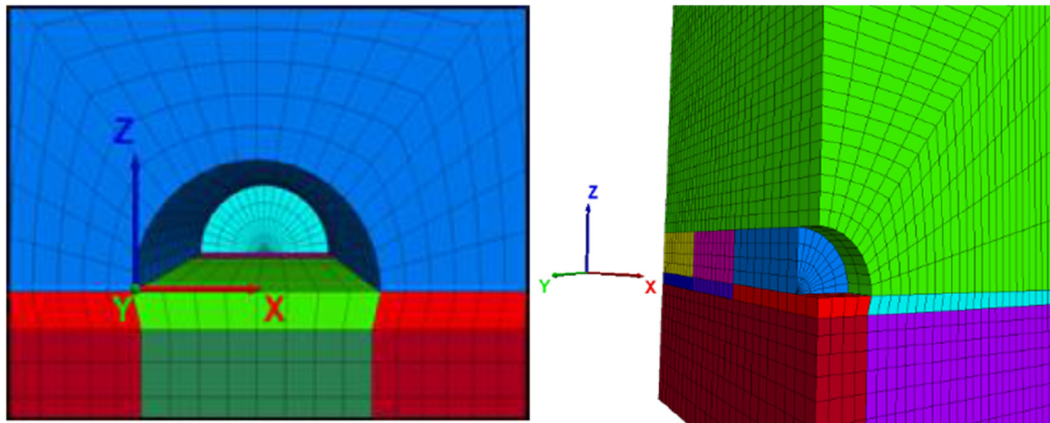


FIGURE 10
Sequential excavation in a tunnel.

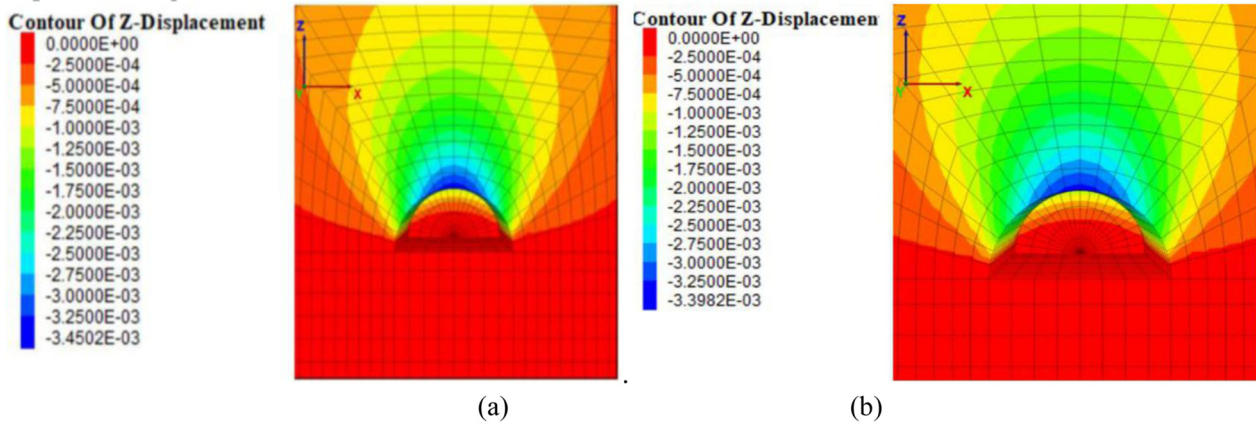


FIGURE 11
Vertical displacement contour of crown without and with support installation: (a) roof movement without support; (b) roof movement with support.

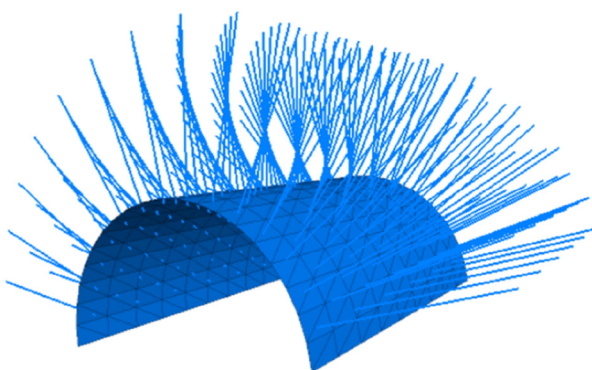
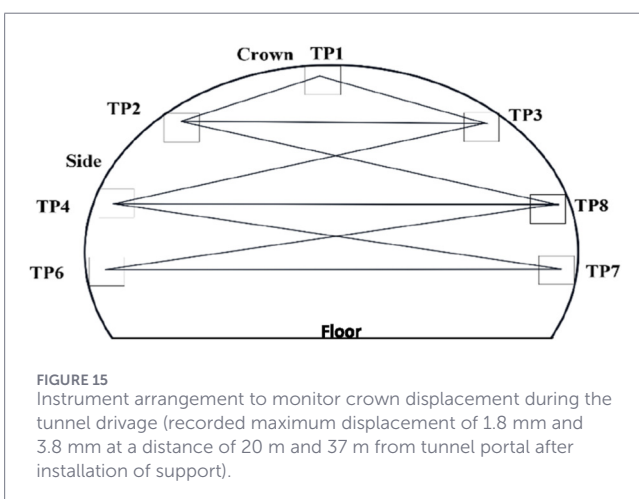
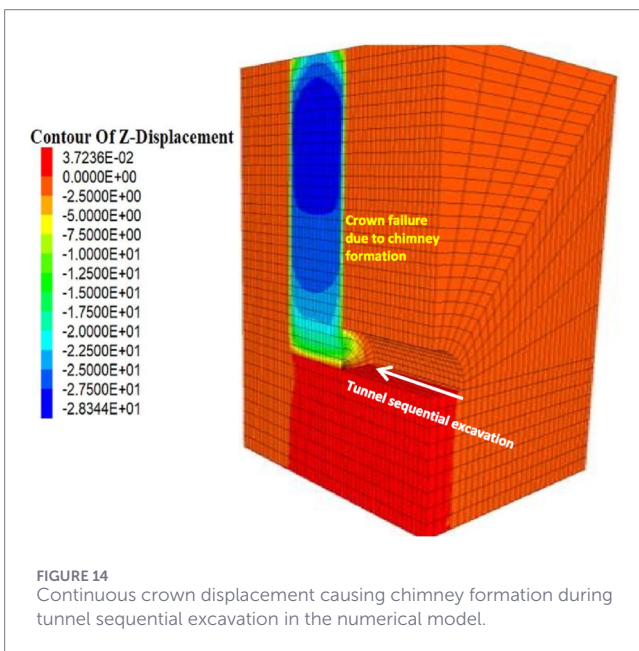


FIGURE 12
Installation of rock bolt and liners in the tunnel numerical model for the simulation.

performance, and broader implications for tunnel design and construction.

The numerical simulation results demonstrate that crown displacement is strongly influenced by the presence of weak and sheared rock mass zones above the tunnel crown, particularly under shallow to moderate overburden conditions. The progressive increase in vertical displacement observed during sequential excavation confirms that stress redistribution and loss of confinement play a dominant role in initiating chimney failure. These findings are consistent with earlier observations that cavity formation is not solely governed by stand-up time concepts but is controlled by localised geological weakness, groundwater conditions, and excavation-induced stress relief.

Comparison between unsupported and supported excavation stages highlights the critical role of timely and adequate support installation. The unsupported tunnel condition exhibited a continuous increase in crown displacement with excavation advance, ultimately leading to the formation of a cavity. In contrast, the supported condition showed a marked reduction in displacement magnitude and deformation rate, indicating that support systems significantly enhance



tunnel stability. However, the occurrence of cavity failure despite the installation of support in weak zones suggests that conventional support measures may be insufficient when applied uniformly, without accounting for localised geological variability.

Field monitoring data obtained from extensometers provided valuable calibration for the numerical model, enabling objective validation of the simulated displacement trends. The close agreement between measured and simulated crown displacements reinforces the reliability of the numerical approach adopted in this study. Importantly, the identification of displacement thresholds beyond which deformation accelerates offers a practical indicator for early warning and adaptive support design during tunnel construction.

The results also emphasise the influence of groundwater conditions on chimney failure. The presence of perched aquifers and water inflow above the crown reduced effective stress and weakened the rock mass, thereby exacerbating deformation and cavity growth. This underscores the necessity of incorporating groundwater effects into both numerical modelling and support design, particularly in Himalayan tunnelling projects where hydrological uncertainty is high.

From a design perspective, the study highlights the need for site-specific and performance-based support strategies rather than reliance on generalised ground classifications alone. The integration of field monitoring, numerical simulation, and geological characterisation provides a robust framework for assessing tunnel stability and optimising support systems in weak ground conditions. Such an approach aligns with modern sustainable tunnelling practices, as it enables minimisation of overbreak, efficient use of support materials, and improved construction safety.

Overall, the findings of this study contribute to a better understanding of chimney failure mechanisms in Himalayan tunnels and demonstrate the effectiveness of combining numerical modelling with field data for evaluating support performance. The proposed approach can be applied to similar tunnelling projects in complex geological environments to enhance stability assessment, support design, and risk mitigation strategies.

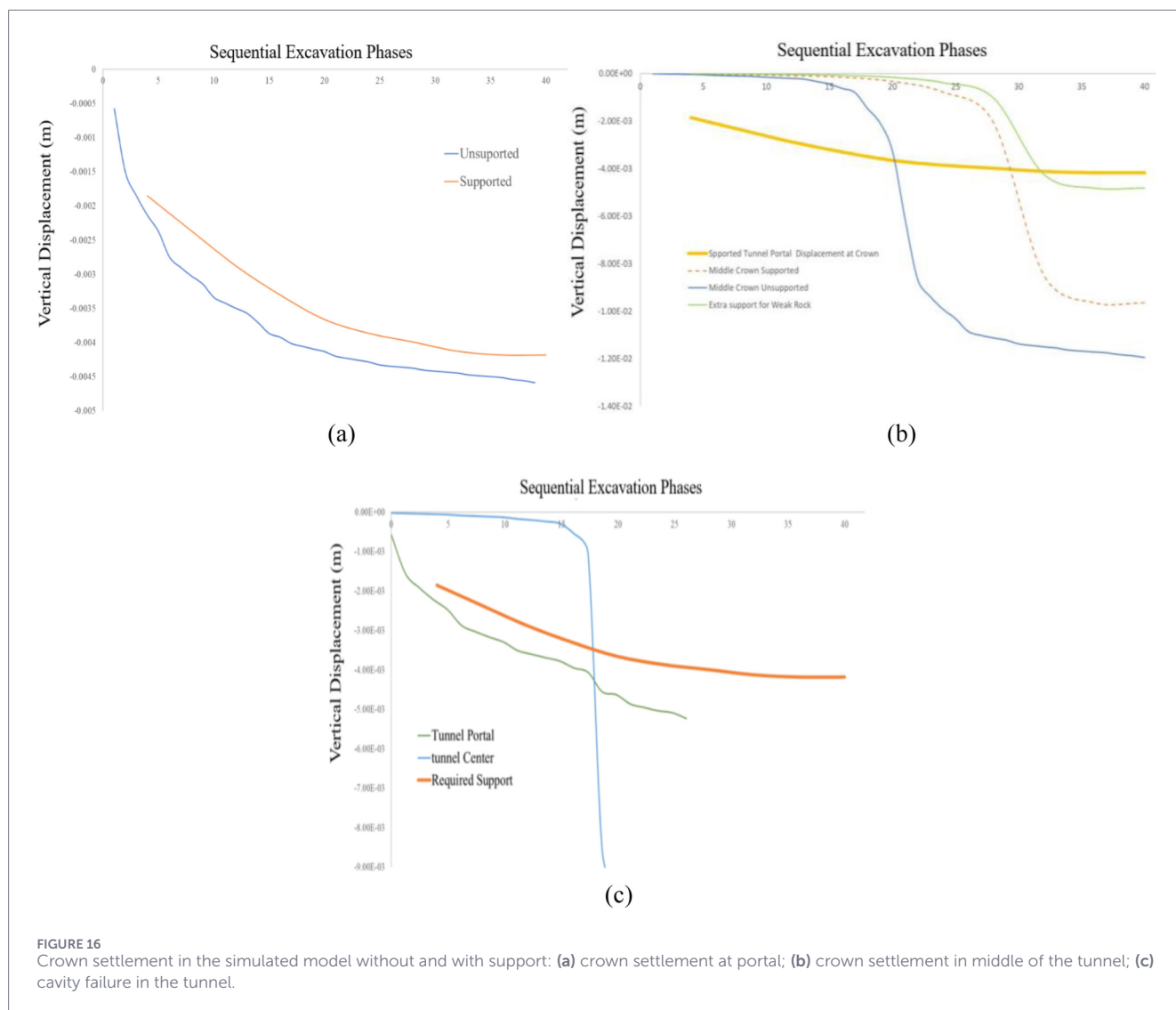


FIGURE 16

Crown settlement in the simulated model without and with support: (a) crown settlement at portal; (b) crown settlement in middle of the tunnel; (c) cavity failure in the tunnel.

7 Conclusion

This study focused on the analysis and remediation of cavity failure during tunnelling in the Himalayas and also assess the efficacy of the existing support system. Numerical modelling of unsupported and supported tunnels in the simulation software, the performance of the support system and its ability to mitigate deformation and stresses was evaluated. Based on the observations, the proposed support system proved to be effective in controlling crown displacement and vertical stresses, indicating its efficiency in maintaining tunnel stability. It was also evident that the support requirements varied for different rock classes, highlighting the importance of adapting the support system to suit the specific geological conditions encountered during tunnelling in the Himalayas. The analysed support system comprising rock bolts, shotcrete, and steel ribs demonstrated effective control of crown displacement and vertical stress concentration, reducing deformation by approximately 40%–55% compared to unsupported conditions, as found from field and simulation results. This study provides valuable insights into the analysis and remediation of cavity

failure during tunnelling in the challenging geological conditions of the Himalayas. The findings emphasize the significance of an appropriate support system design and the consideration of pore water pressure effects to ensure safe and successful tunnel construction in the region as per the changing ground conditions.

Data availability statement

The raw data supporting the conclusions of this article will be made available by the authors, without undue reservation.

Author contributions

RK: Conceptualization, Data curation, Investigation, Methodology, Resources, Software, Validation, Visualization, Writing – review and editing, Formal Analysis. AsK: Conceptualization, Data curation, Formal Analysis,

Investigation, Methodology, Resources, Software, Validation, Visualization, Writing – review and editing, Supervision, Writing – original draft. AbK: Conceptualization, Data curation, Investigation, Methodology, Resources, Visualization, Writing – original draft, Writing – review and editing, Software, Validation. BP: Methodology, Formal analysis, Validation, Writing – review and editing. SR (5th author): Data curation, Formal Analysis, Writing – review and editing, Conceptualization, Investigation, Methodology, Resources, Visualization, Writing – original draft. SR (6th author): Methodology, Formal analysis, Validation, Writing – review and editing. KS: Data curation, Formal Analysis, Supervision, Validation, Writing – review and editing, Funding acquisition, Project administration. KZ: Data curation, Formal Analysis, Funding acquisition, Supervision, Validation, Writing – review and editing. AZ: Data curation, Formal Analysis, Funding acquisition, Supervision, Validation, Writing – review and editing. JS: Data curation, Formal Analysis, Supervision, Validation, Writing – review and editing. ZR: Data curation, Formal Analysis, Supervision, Validation, Writing – review and editing.

Funding

The author(s) declared that financial support was not received for this work and/or its publication.

References

- Abbas, N., Li, K., Fissah, Y., Lei, W., Emad, M. Z., Chandradas, N. S., et al. (2024). Stress-deformation and stability challenges in Himalayan tunnels: impact of geological discontinuities. *Discov. Mater.* 4, 72. doi:10.1007/s43939-024-00144-z
- Ahmed, A., Mishra, S. K., Azad, M. A., Alquamar, C., Singh, T. N., Ansari, A., et al. (2025). Prediction of tunnel ground deformation – a case study from Western Himalaya, India. Results in. *Earth Sci.* 3, 100052. doi:10.1016/j.rines.2024.100052
- Barton, N., Lien, R., and Lunde, J. (1975). “Estimation of support requirements for underground excavations,” in *Proc. Sixteenth symp. On rock mechanics* (Minnesota, U.S.A.: Univ. of Minnesota), 163–177.
- Beg, Y., Singh, V., Kundu, S., and Bhowmik, R. (2025). “Tunneling challenges in Himalayan region—A review,” in *Proceedings of 9IYGEC 2023* (Singapore: Springer Nature), 2, 207–217. doi:10.1007/978-981-97-6988-9_21
- Bieniawski, Z. T. (1993). “Classification of rock masses for engineering: the RMR system and future trends,” in *Rock testing and site characterization*. Editor J. A. Hudson (Oxford: Pergamon), 553–573.
- Chen, L., Wang, Z. F., Wang, Y., Xitong, B., and Lai, J. (2022). Characteristics and failure analysis of a railway tunnel collapse influenced by cavity in phyllite strata. *Eng. Fail. Anal.* 142, 106794. doi:10.1016/j.engfailanal.2022.106794
- Diwakar, K. C., Gautam, K., Dangi, D., Kadel, S., and Hu, L. (2022). Challenges in tunneling in the Himalayas: a survey of several prominent excavation projects in the Himalayan Mountain range of south Asia. *Geotechnics* 2, 802–824.
- Huang, F., Zhao, L. H., Ling, T. H., and Yang, X. L. (2017). Rock mass collapse mechanism of concealed karst cave beneath deep tunnel. *Int. J. Rock Mech. Min. Sci.* 91, 133–138. doi:10.1016/j.ijrmm.2016.11.017
- Huang, H., Zhang, D., and Huang, Z. (2022). Resilience of city underground infrastructure under multi-hazards impact: from structural level to network level. *Resilient Cities Struct.* 1 (2), 76–86. doi:10.1016/j.rcns.2022.07.003
- Koopialipoor, M., Asteris, G., Salih, M. A., Alexakis, D. E., Mamou, A., and Armaghani, D. J. (2022). Introducing stacking machine learning approaches for the prediction of rock deformation. *Transp. Geotech.* 34, 100756.
- Kumar, R. (2023). *Analysis and remediation of cavity failure during tunnelling in the Himalayas*. M.Tech thesis. Dhanbad, India: Indian Institute of Technology (Indian School of Mines).
- Lauffer, H. (1958). Gebirgsklassifizierung für den Stollenbau. *Geol. Bauwesen* 24, 46–51.
- Leu, S. S., Chen, C. N., and Chang, S. L. (2001). Data mining for tunnel support stability: neural network approach. *Automation Constr.* 10, 429–431. doi:10.1016/S0926-5805(00)00078-9
- Li, J., Fang, Y., Liu, C., Zhang, Y., and Lu, W. (2020). Performance investigation of tunnel lining with cavities around surrounding rocks. *Adv. Civ. Eng.* 2020, 1364984. doi:10.1155/2020/1364984
- Liu, X. R., Li, D., Zhong, Z. L., and Wu, Q. (2013). Research on collapse mechanism and disaster treatment of mayakou tunnel by the action of fluid-structure interaction (FSI). *Disaster Adv.* 5 (4), 903–908.
- Liu, X. Z., Liu, F., and Song, K. Z. (2022). Mechanism analysis of tunnel collapse in a soft-hard interbedded surrounding rock mass: a case study of the yangshan tunnel in China. *Eng. Fail. Anal.* 138, 106304. doi:10.1016/j.engfailanal.2022.106304
- Liu, J., Xie, Q., Han, B., Wang, J., Lv, G., and Luo, X. (2024). Experimental and numerical study of the failure mechanism and stability of tunnel linings under different cavity conditions. *Eng. Fail. Anal.* 162, 108412. doi:10.1016/j.engfailanal.2024.108412
- Nguyen, N. H. T., Bui, H. H., Nguyen, G. D., and Kodikara, J. (2017). A cohesive damage-plasticity model for DEM and its application for numerical investigation of soft rock fracture properties. *Int. J. Plast.* 98, 175–196. doi:10.1016/j.jiplas.2017.07.008
- Rabczewicz, L. (1973). Principles of dimensioning the supporting system for the new Austrian tunnelling method. *Water Power* 25, 88–93.
- Rajput, A., Kaushik, A., Iqbal, M. A., and Gupta, N. K. (2023). Non-linear FE investigation of subsurface tunnel with GFRP protection against internal blast. *Int. J. Impact Eng.* 172, 104423. doi:10.1016/j.ijimpeng.2022.104423
- Schmidt, F., Sagaseta, C., and Konietzky, H. (2010). “3D analysis of a micropile umbrella for stabilizing the tunnel face of a NATM tunnel,” in *Numerical methods in geotechnical engineering – Benz and nordal*, 749–753.
- Shen, Y. S., Gao, B., Yang, X. M., and Tao, S. (2014). Seismic damage mechanism and dynamic deformation characteristic analysis of mountain tunnel after wenchuan earthquake. *Eng. Geol.* 180 (8), 85–98. doi:10.1016/j.enggeo.2014.07.017
- Spyridis, P., and Bergmeister, K. (2024). Sustainable tunnel design: concepts and examples of reducing greenhouse gas emissions through basic engineering assumptions. *Tunn. Undergr. Space Technol.* 152, 105886. doi:10.1016/j.tust.2024.105886
- Upadhyay, S., Kaushal, V., Baishta, D., and Bhakat, S. K. (2023). Mitigating loose rock fall and cavity formation in Adit-2 tunnel of rammam III hydroelectric project in Himalayas, India: challenges and solutions. *IOP Conf. Ser. Earth Environ. Sci.* 1249, 012014. doi:10.1088/1755-1315/1249/1/012014
- Yang, W., Zheng, J., Zhang, R., and Liu, H. (2021). An empirical model for characterizing 3D deformation at the face of shield tunnel in soft clay. *Tunn. Undergr. Space Technol.* 112, 103862. doi:10.1016/j.tust.2021.103862

Conflict of interest

The author(s) declared that this work was conducted in the absence of any commercial or financial relationships that could be construed as a potential conflict of interest.

Generative AI statement

The author(s) declared that generative AI was not used in the creation of this manuscript.

Any alternative text (alt text) provided alongside figures in this article has been generated by Frontiers with the support of artificial intelligence and reasonable efforts have been made to ensure accuracy, including review by the authors wherever possible. If you identify any issues, please contact us.

Publisher's note

All claims expressed in this article are solely those of the authors and do not necessarily represent those of their affiliated organizations, or those of the publisher, the editors and the reviewers. Any product that may be evaluated in this article, or claim that may be made by its manufacturer, is not guaranteed or endorsed by the publisher.